The EMBO Journal (2011) 30, 2219–2232 | © 2011 European Molecular Biology Organization | All Rights Reserved 0261-4189/11
www.embojournal.org

THE EMBO JOURNAL

Aging and chronic DNA damage response activate a regulatory pathway involving miR-29 and p53

Alejandro P Ugalde[1], Andrew J Ramsay[1], Jorge de la Rosa[2], Ignacio Varela[1], Guillermo Mariño[1], Juan Cadiñanos[2], Jun Lu[3], José MP Freije[1] and Carlos López-Otín[1,*]

[1]Departamento de Bioquímica y Biología Molecular, Instituto Universitario de Oncología, Universidad de Oviedo, Oviedo, Spain, [2]Laboratorio de Medicina Molecular, Instituto de Medicina Oncológica y Molecular de Asturias, Oviedo, Spain and [3]Department of Genetics, Yale University, Yale Stem Cell Center, New Haven, CT, USA

Aging is a multifactorial process that affects most of the biological functions of the organism and increases susceptibility to disease and death. Recent studies with animal models of accelerated aging have unveiled some mechanisms that also operate in physiological aging. However, little is known about the role of microRNAs (miRNAs) in this process. To address this question, we have analysed miRNA levels in *Zmpste24*-deficient mice, a model of Hutchinson–Gilford progeria syndrome. We have found that expression of the miR-29 family of miRNAs is markedly upregulated in *Zmpste24*$^{-/-}$ progeroid mice as well as during normal aging in mouse. Functional analysis revealed that this transcriptional activation of miR-29 is triggered in response to DNA damage and occurs in a p53-dependent manner since *p53*$^{-/-}$ murine fibroblasts do not increase miR-29 expression upon doxorubicin treatment. We have also found that miR-29 represses Ppm1d phosphatase, which in turn enhances p53 activity. Based on these results, we propose the existence of a novel regulatory circuitry involving miR-29, Ppm1d and p53, which is activated in aging and in response to DNA damage.

The EMBO Journal (2011) **30,** 2219–2232. doi:10.1038/emboj.2011.124; Published online 26 April 2011
Subject Categories: RNA; genome stability & dynamics; molecular biology of disease
Keywords: cancer; microRNA; phosphatase; progeria; tumour suppressor

Introduction

Aging is a complex process that progressively compromises most of the biological functions of the organism, resulting in an increased susceptibility to disease and death. Although a considerable effort has been made to unveil the causes of aging, there is no consensus theory to completely explain this process (Vijg and Campisi, 2008). Nevertheless, there is some agreement that a common feature of aging is the progressive accumulation of cellular damage. Several stressors have been proposed to contribute to this cell damage, such as oxidative reactions, telomere attrition, or the decline of DNA repair and protein turnover systems (Kirkwood, 2005). Evidence for the association of DNA damage with aging is supported by the identification of gene mutations that lead to an accelerated development of many age-related features. Most of these mutations were originally found in genes encoding proteins directly implicated in DNA repair (Hoeijmakers, 2009), but recent studies have revealed that alterations in other processes that affect genomic integrity, such as nuclear envelope formation and dynamics, are also responsible for the development of premature aging syndromes (Hasty *et al*, 2003; Cadinanos *et al*, 2005; Broers *et al*, 2006). Thus, mice with mutations in lamin A or deficient in the Zmpste24 metalloprotease involved in its maturation, display multiple features of premature aging (Osorio *et al*, 2009). This phenotype is associated with an increased genomic instability as a consequence of the nuclear envelope network disruption and is supported by the transcriptional upregulation of p53 target genes and the decline in the function of somatic stem cells (Pendas *et al*, 2002; Varela *et al*, 2005; Espada *et al*, 2008). On this basis, it has been proposed that the same mechanisms that detect damage and protect cells from malignant transformation may have a deleterious effect in aged tissues, thereby providing a good example of the principle of antagonistic pleiotropy (Campisi, 2005; Kirkwood, 2005).

Over the last decade, miRNAs have emerged as new and fundamental actors in the gene regulation scenario. These ~21–24 nucleotide RNA molecules are able to bind to specific sites typically present in the 3′-UTR region of their target genes and mediate either mRNA decay or translational blockade (Flynt and Lai, 2008). Although the function of only a small percentage of the identified miRNAs is known, computational predictions have estimated that at least 20–30% of transcripts are susceptible to miRNA-mediated regulation (Lewis *et al*, 2005). miRNAs were initially associated with development regulation, but numerous studies have revealed that these small RNA molecules have essential roles in a wide variety of physiological and cellular processes (Bushati and Cohen, 2007). As a consequence, miRNA dysregulation is a common feature found in cancer, and several members of this family of regulatory RNAs have been proposed to act as oncogenes or tumour suppressors (He *et al*, 2007; Shenouda and Alahari, 2009; Garzon *et al*, 2009a).

At present, very little is known about the implication of miRNAs during mammalian aging. In contrast, several miRNAs have been associated with aging in *Caenorhabditis elegans* and it has been shown that knockdown of *lin-4* miRNA extends lifespan in these nematodes (Boehm and Slack, 2005; Williams *et al*, 2007). In vertebrates, profiling studies in liver and skeletal muscle from aged mice have revealed changes in miRNA expression during aging,

*Corresponding author. Departamento de Bioquímica y Biología Molecular, Facultad de Medicina, Universidad de Oviedo, Fernando Bongera s/n Edificio Santiago Gascon, Oviedo 33006, Spain. Tel.: +34 985 104201; Fax: +34 985 103564; E-mail: clo@uniovi.es

Received: 26 July 2010; accepted: 30 March 2011; published online: 26 April 2011

although no differences have been identified in lung (Williams *et al*, 2007; Drummond *et al*, 2008; Maes *et al*, 2008). Additionally, several miRNAs have been found to be dysregulated in the Ames dwarf mice, and miR-27 has been proposed to have a role in the delayed aging observed in these mice (Bates *et al*, 2010). However, to date, no such studies have been performed in premature aging mice. In this work, we have evaluated for the first time the miRNA expression levels in a mouse model of human Hutchinson–Gilford progeria. We report that the expression of the miR-29 family of miRNAs is dysregulated in both pathological and physiological aging. In addition, we have found that miR-29 miRNAs form part of a new signalling pathway involving the Ppm1d/Wip1 phosphatase and the p53 tumour suppressor, which is activated in aging and during chronic DNA damage response.

Results

Dysregulation of miRNAs in Zmpste24$^{-/-}$ progeroid mice

To identify miRNAs that could be implicated in normal or pathological aging processes, we first analysed the miRNA transcriptome of *Zmpste24*-null mice, a mouse model of Hutchinson–Gilford progeria that exhibits accelerated aging and recapitulates many symptoms of normal aging (Varela *et al*, 2005). To this purpose, we used a bead-based flow cytometric platform covering the complete set of mouse and human miRNAs to profile miRNA expression levels in liver from *Zmpste24*-deficient mice (Lu *et al*, 2005). This analysis revealed the differential expression of a series of miRNAs, which were significantly upregulated or downregulated in these progeroid mice. Interestingly, three of the miRNAs whose expression levels were altered in *Zmpste24*-deficient mice (miR-29a, miR-29b and miR-29c) belong to the same family (Figure 1A). Accordingly, we next proceeded to further validate these flow cytometry-based miR-29 expression results by stem loop quantitative PCR miRNA assays. As shown in Figure 1B, we confirmed the upregulation of all three members of the miR-29 family in *Zmpste24*$^{-/-}$-deficient mice, with values for miR-29a, -29b and -29c being 1.6-, 2.7- and 1.6-fold increased when compared with normal tissues. As a control, we assayed in parallel the expression levels of miR-23b, which shows no changes between normal and mutant liver in the array-based profiling analysis (Figure 1B).

Next, we extended the miRNA expression study to other tissues from *Zmpste24*$^{-/-}$ mice, such as muscle, which displays considerable alterations in this mouse model (Pendas *et al*, 2002). As shown in Figure 1C, miR-29 levels were dramatically altered in this tissue, as assessed by the finding of a 9.7-fold induction for miR-29b in *Zmpste24*$^{-/-}$ mice (Figure 1C). Likewise, miR-29a and -29c levels were also markedly increased in muscle from *Zmpste24*$^{-/-}$ mice when compared with wild-type littermates (5.1- and 4.4-fold, respectively). Because *Zmpste24*-null mice phenocopy many alterations characteristic of normal aging, we next asked whether these miRNAs could also be dysregulated in aged mice. To evaluate this hypothesis, we analysed miR-29 expression levels in tissues from 2-year-old mice. As can be seen in Figure 1B and C, the expression levels of miR-29a, -29b and -29c in liver and muscle from wild-type

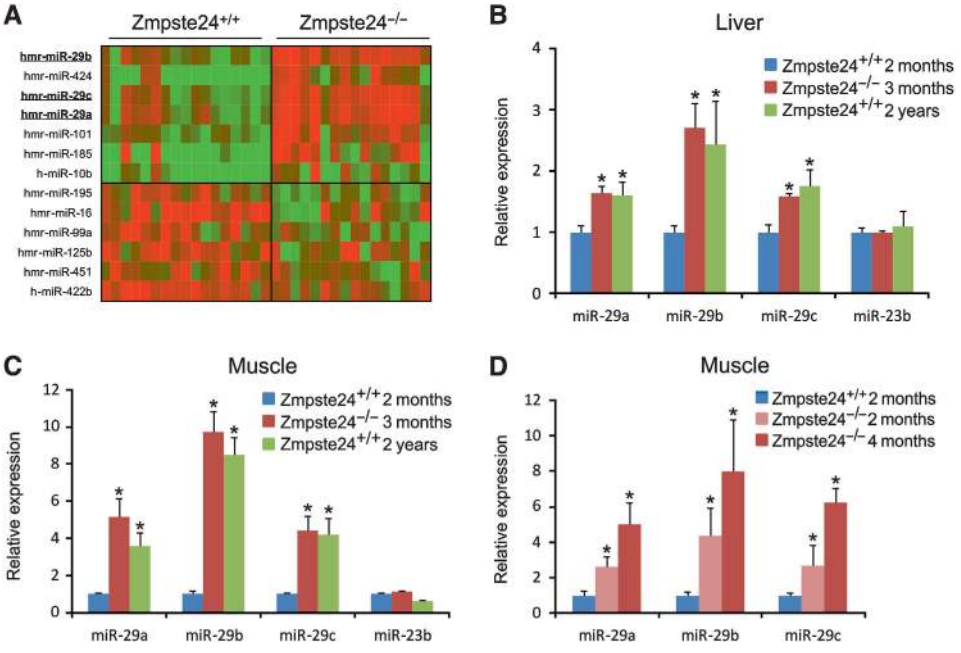

Figure 1 miRNA expression analysis in tissues from *Zmpste24*$^{-/-}$ mice. (**A**) A total of 17 and 16 *Zmpste24*$^{-/-}$ and *Zmpste24*$^{+/+}$ liver samples were analysed through a bead-based flow cytometry platform that covers the complete set of human and mouse miRNAs. miRNAs with significant fold induction were plotted as a colour heat map, with the miR-29 family miRNAs underlined (P-value < 0.05, $0.75 \geqslant$ fold induction $\geqslant 1.25$). (**B**) miR-29a, -29b and -29c upregulation in *Zmpste24*$^{-/-}$ was confirmed through stem loop qPCR in liver samples. Expression analysis in liver from aged mice shows similar levels of miR-29 miRNAs than in samples from *Zmpste24*$^{-/-}$ mice. As a control, levels of miR-23b that shows no changes in the profiling study were analysed. (**C**) qPCR analysis of the miR-29 family in muscle revealed eight-fold induction in samples from *Zmpste24*$^{-/-}$ and aged *Zmpste24*$^{+/+}$, compared with young *Zmpste24*$^{-/-}$. (**D**) Correlation between miR-29 levels and phenotype development in *Zmpste24*$^{-/-}$ muscle samples. For all the experiments, a minimum of three animals were analysed. *Significantly different from 2-month-old wild-type mice, $P < 0.05$.

aged mice were higher than those of young mice and very similar to those present in the same tissues from 2-month-old *Zmpste24*$^{-/-}$ mice (3.6-, 8.5- and 4.2-fold, respectively). Finally, we examined the putative correlation between miR-29 levels and phenotype development in *Zmpste24*$^{-/-}$ muscle samples, with the finding that 2-month-old mice, which are almost indistinguishable from their wild-type littermates, present significantly lower levels of miR-29 compared with 4-month-old mice, which display the most severe phenotype, as assessed by an extensive hair and weight loss and a prominent kyphosis (Figure 1D). This observation suggests that the miR-29 family upregulation is an early event in the development of *Zmpste24*-deficient mice phenotype rather than a consequence of the multiple alterations present in these progeroid mice.

Additionally, we analysed the putative changes in miR29-expression levels in some available tissues from progeroid mice deficient in other genes implicated in DNA repair, including *XPF*- (Tian *et al*, 2004), *CSB/XPA*- (van der Pluijm *et al*, 2007) and *ATM*-deficient mice (Elson *et al*, 1996), as well as *ATR-Seckel* mice (Murga *et al*, 2009). However, no significant changes in the miR-29 family were found in any of the DNA repair deficiency models. Overall, these data would suggest that the miR-29 increase in the *Zmpste24*$^{-/-}$ model is dependent upon a chronic DNA damage due to a very specific genotoxic stress caused by nuclear envelope dysfunction, but not initiated in response to intrinsic genomic stress derived from repair machinery impairment. Taken together, these data associate the miR-29 family with normal and pathological aging, and reinforce the relevance of *Zmpste24*-null mice as a model to study the molecular links between miRNA dysregulation and aging processes.

miR-29 induction is linked to DNA damage response

We have previously shown that *Zmpste24*-null mice present nuclear abnormalities linked to altered chromatin architecture and p53 pathway activation, a situation which suggests the existence of a chronic response to genomic damage (Liu *et al*, 2005; Varela *et al*, 2005; Espada *et al*, 2008). On this basis, we hypothesized that the miR-29 upregulation observed in aging tissues could be triggered as a result of genomic damage. As a first step to evaluate this hypothesis, we analysed miR-29 expression during successive passages of *Zmpste24*$^{-/-}$ primary fibroblasts until they reached replicative senescence. As shown in Figure 2A, miR-29a, -29b and -29c levels are consistently higher at passage six and correlate with the significant accumulation of senescence-associated β-galactosidase (SA-βGal)-positive cells and a considerable increase in the levels of the DNA damage marker γ-H2AX in comparison to initial passage controls (Figure 2C and D). To evaluate whether this phenomenon is an exclusive feature of mutant mice fibroblasts, we extended the analysis to wild-type fibroblasts, finding that these cells undergo the same grade of miR-29 upregulation at serial passage six (Figure 2B) and show no significant differences at passage one or six compared with *Zmpste24*$^{-/-}$ fibroblasts under the same

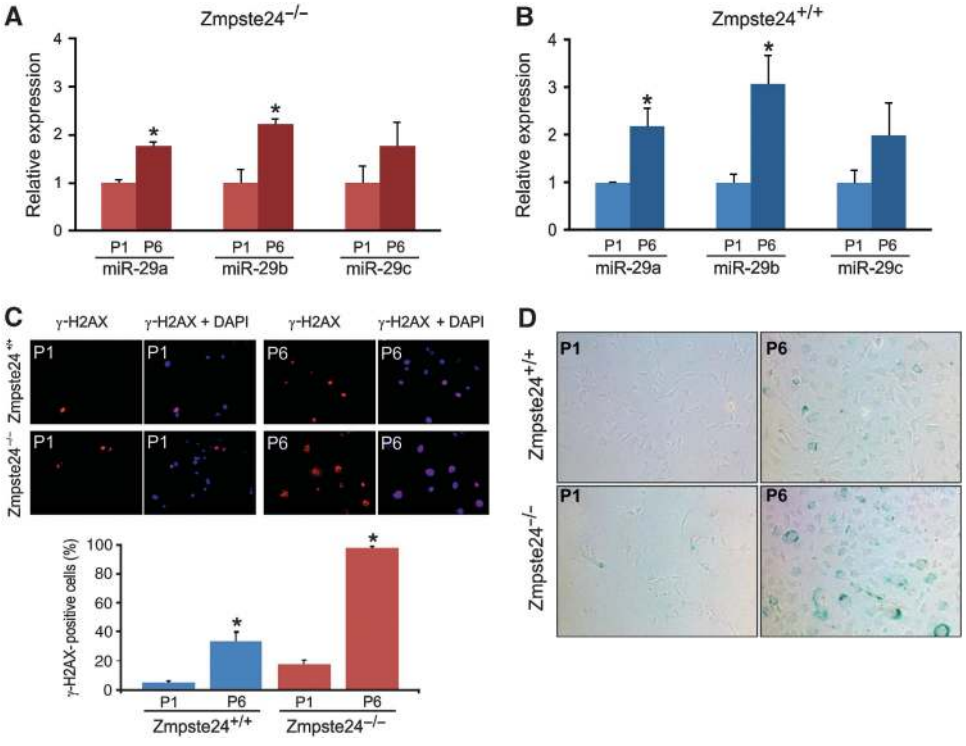

Figure 2 miR-29 expression is associated with DNA damage and cell senescence. Levels of miR-29 increase with serial passages of *Zmpste24*$^{-/-}$ (**A**) and *Zmpste24*$^{+/+}$ (**B**) primary ear fibroblasts in culture. Total RNA from three independent *Zmpste24*$^{-/-}$ and *Zmpste24*$^{+/+}$ fibroblast cell lines was extracted at passages 1 and 6 and the miR-29a, -29b and -29c levels were analysed by qPCR. *Significantly different from passage 1 fibroblasts, $P<0.05$. (**C**) Representative images and quantification (lower chart) of γ-H2AX staining in the three *Zmpste24*$^{-/-}$ and *Zmpste24*$^{+/+}$ fibroblast cell lines at passages 1 and 6. *Significantly different from passage 1 fibroblasts, $P<0.05$. (**D**) Senescence-associated β-galactosidase activity (SA-βGAL) representative images from *Zmpste24*$^{-/-}$ and *Zmpste24*$^{+/+}$ primary fibroblasts at passages 1 and 6. Both wild-type and *Zmpste24*-mutant primary fibroblasts show an increase in γ-H2AX foci and SA-βGal activity at passage 6, evidencing the genotoxic stress induced by the *in vitro* serial passage of primary fibroblasts.

culture conditions. Senescence and DNA damage studies in wild-type fibroblasts demonstrated that although there is a progressive accumulation of SA-βGal and γ-H2AX during serial passaging, which clearly correlates miR-29 upregulation with cellular conditions of increased DNA damage, both markers are significantly increased in *Zmpste24*-deficient fibroblasts (Figure 2C and D). This observation can conceivably be attributed to multiple additional pathway alterations present in the mutant fibroblasts.

To clarify further if genomic damage is responsible for this miR-29 activation, growing wild-type fibroblasts were treated with doxorubicin, a DNA topoisomerase inhibitor that generates a DNA damage that is difficult to repair and induces the expression of miRNAs implicated in the p53 pathway, such as miR-34 (L'Ecuyer *et al*, 2006; Rokhlin *et al*, 2008). As can be seen in Figure 3A, miR-29 expression was induced in wild-type fibroblasts, after 24 h treatment with 1 μM doxorubicin. In contrast, treatment with drugs that induce transient oxidative damage, such as H_2O_2, or UV-like lesions, like those attributed to 4-nitroquinolone-1-oxide (4-NQO) (Eller *et al*, 1996) failed to induce the expression of this family of miRNAs (Figure 3B), suggesting that the main stimulus for miR-29 transcriptional activation is the accumulation of chronic, difficult to repair DNA lesions. To further explore whether the observed miR-29 upregulation is associated with p53 signalling activation, we performed similar experiments with $p53^{-/-}$ fibroblasts, with the finding that the deletion of p53 abolishes miR-29 induction after doxorubicin treatment (Figure 3A). Moreover, and in agreement with these data, we have found that *p53*-deficient primary mouse fibroblasts fail to upregulate miR-29 expression during successive passages of cell culture, providing further evidence of the connection between p53, miR-29 and replicative senescence, as $p53^{-/-}$ fibroblasts never enter a non-growing senescent phase (Harvey *et al*, 1993; Supplementary Figure S1A). Further, we extended these experiments to fibroblasts defective in ATM or containing the ATR-Seckel mutation, demonstrating that disruption of both DNA damage response pathways abolishes miR-29 upregulation under an equivalent dosage of doxorubicin (Supplementary Figure S1A). Interestingly, high concentrations of doxorubicin induced miR-29 transcriptional activation even in the absence of functional ATM or ATR proteins, indicating that other regulatory mechanisms are operating under these conditions.

Having established that p53 deficiency in fibroblasts attenuates the increase of the miR-29 family in response to doxorubicin-induced DNA damage, we next analysed if p53 is required for the initiation of promoter activity of both the hsa-miR-29b-1∼29a and hsa-miR-29b-2∼29c clusters. Accordingly, ∼4 kb of the promoter sequence of both

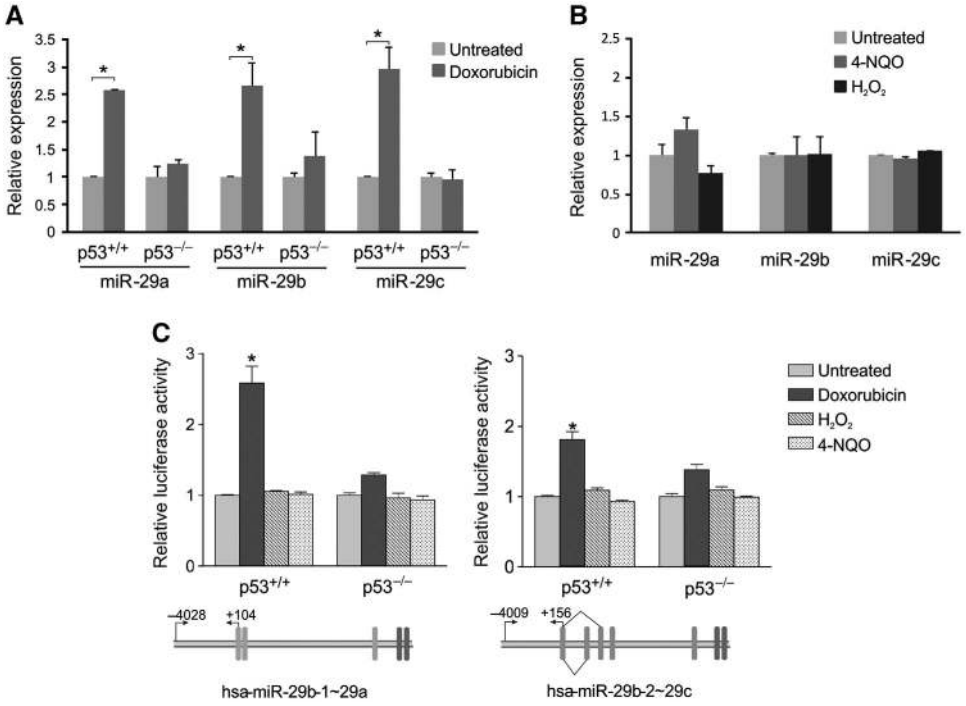

Figure 3 miR-29 induction is linked to DNA damage response. (**A**) miR-29 expression is activated during DNA damage in a p53-dependent manner. Primary ear fibroblasts from $p53^{+/+}$ and $p53^{-/-}$ mice were treated for 24 h with doxorubicin or left untreated in parallel, and miR-29 expression was analysed by qPCR ($n=2$ biological replicates). (**B**) Transient damage induced by H_2O_2 or UV-like lessons caused by 4-nitroquinolone-1-oxide (4-NQO) show no effect on miR-29 transcription. Primary ear fibroblasts were treated with 80 μM H_2O_2 or 0.8 μM 4-NQO for 24 h and miR-29 levels were analysed by qPCR ($n=2$ biological replicates). Untreated samples in (**A**) and (**B**) were taken at the same time points as in treated cells. (**C**) Transcriptional regulation of miR-29 promoters. Approximately 4 kb of the promoter sequence of both hsa-miR-29b-1∼29a and hsa-miR-29b-2∼29c clusters were cloned upstream the firefly luciferase coding sequence of the pGL3-basic plasmid (diagrams below the chart). Promoter constructs were transfected in wild-type *or* $p53^{-/-}$ HCT-116 cells and treated with 1 μM doxorubicin or left untreated for 36 h. In all transfections, a plasmid expressing *Renilla* luciferase was included for normalization. The normalized luciferase activity relative to the untreated sample is represented. p53 deficiency abolishes or strongly reduces the promoter activity of hsa-miR-29b-1∼29a and hsa-miR-29b-2∼29c upon doxorubicin treatment, respectively. Additionally, 4-NQO and H_2O_2 treatments were included as a negative control. *Significantly different from the indicated condition, $P<0.05$.

hsa-miR-29b-1∼29a and hsa-miR-29b-2∼29c clusters were cloned upstream the firefly luciferase coding sequence of the pGL3-basic plasmid (Figure 3C, lower panels). Promoter constructs were transfected in parallel with a *Renilla* luciferase expressing construct (normalization control) into wild-type or $p53^{-/-}$ HCT-116 cells and treated with 1 μM doxorubicin or left untreated for 36 h. In complete agreement with quantitative PCR experiments of wild-type mouse fibroblasts exposed to various DNA damaging agents (Figure 3A and B), only doxorubicin treatment was able to activate promoter activity of the hsa-miR-29b-1∼29a and hsa-miR-29b-2∼29c clusters in wild-type HCT-116 cells (Figure 3C, left side of upper panels). Importantly, in a further confirmation of experiments in *p53*-deficient fibroblasts, absence of p53 in the HCT-116 cell line abolished doxorubicin-stimulated promoter activity of the hsa-miR-29b-1∼29a and hsa-miR-29b-2∼29c clusters (Figure 3C, right side of upper panels). Collectively, these experiments indicate that miR-29 transcriptional induction in response to chronic DNA damage is dependent on p53 signalling, an observation that is supported by the study made by Tarasov *et al* (2007) showing that miR-29a is a direct transcriptional target for p53.

Identification of miR-29 targets of potential interest in aging processes

To try to establish the specific role of miR-29 miRNAs in normal and pathological aging, we next performed a computational search of candidate targets that could be subjected to translational repression by members of this miRNA family. Combining the results yielded by the different predictive software available, we first elaborated a list of genes containing putative miR-29 binding sites in their 3′-UTRs and then performed luciferase assays to validate the predicted targets. To this end, the 3′-UTRs of each candidate gene were cloned upstream the ORF of *Renilla* luciferase and the luminescence emission was measured after transfection in HEK-293 cells together with miR-29 precursor molecules or a control miRNA. The different targets showing more than a 50% repression ratio between the miRNA control and any of the miR-29 miRNAs are shown in Figure 4A. Interestingly, all three miR-29 family members exhibited similar activity in the repression ratio of the different targets. These targets include protein phosphatases such as Ppm1d (also called Wip1) and Dusp2, the interferon-inducible protein Ifi30, the transcriptional repressor Hbp1, the prelamin A interacting protein Narf, the Adamts18 metalloproteinase and the Mycn proto-oncogene (Figure 4B). To further validate these findings, we performed similar luciferase-based experiments with the mutated forms of the 3′-UTR of *Narf* and *Ppm1d*, in which we generated a mismatch in the seed region of the putative binding site for miR-29 miRNAs (Figure 5A). We selected these two targets because, in addition to their potential functional relevance in the analysed process, both have a unique binding site for miR-29, which facilitates the mutagenesis experiments and simplifies the analysis of the repression effects. In both mRNAs, the disruption of the

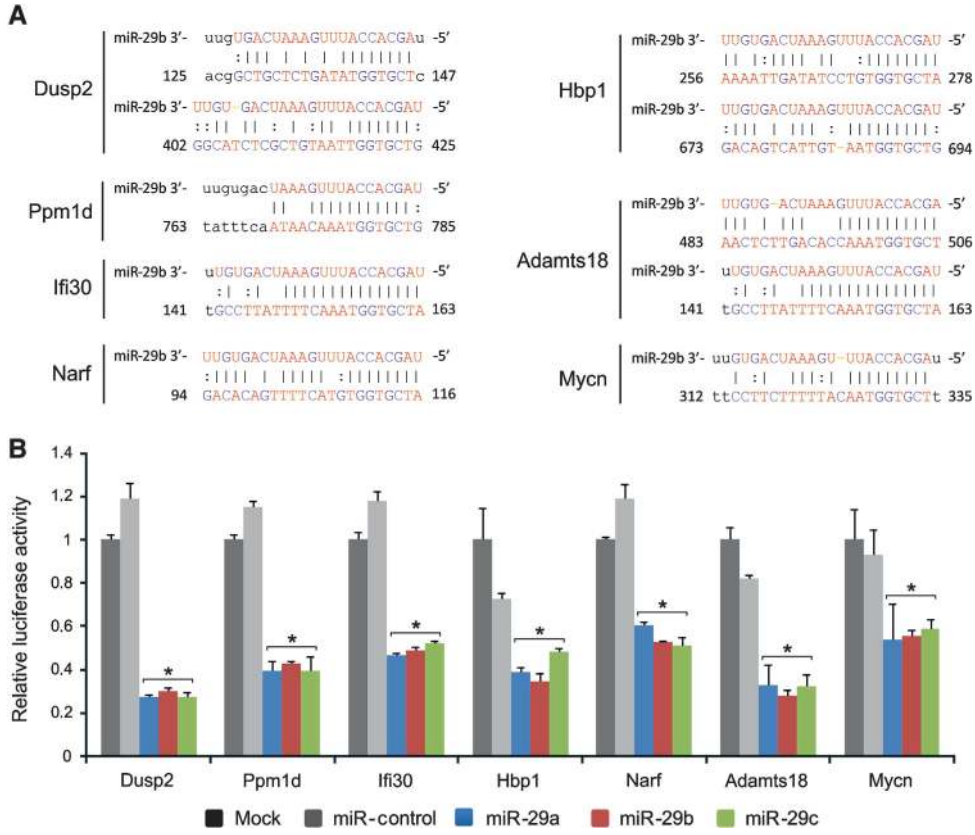

Figure 4 miR-29 target prediction and validation. (**A**) Pairwise alignment of predicted miR-29 targets. Base pair numbers on each 3′-UTR are indicated. (**B**) Luciferase assays in HEK-293 cells. The 3′-UTR of each predicted target was cloned downstream of the ORF of *Renilla* luciferase and transfected into HEK-293 cells alone or together with miR-29a, -29b or -29c or a control miRNA. Data were normalized to the firefly luciferase and experiments were carried out in triplicate. *Significantly different from HEK-293 cells transfected with no miRNA, $P<0.05$.

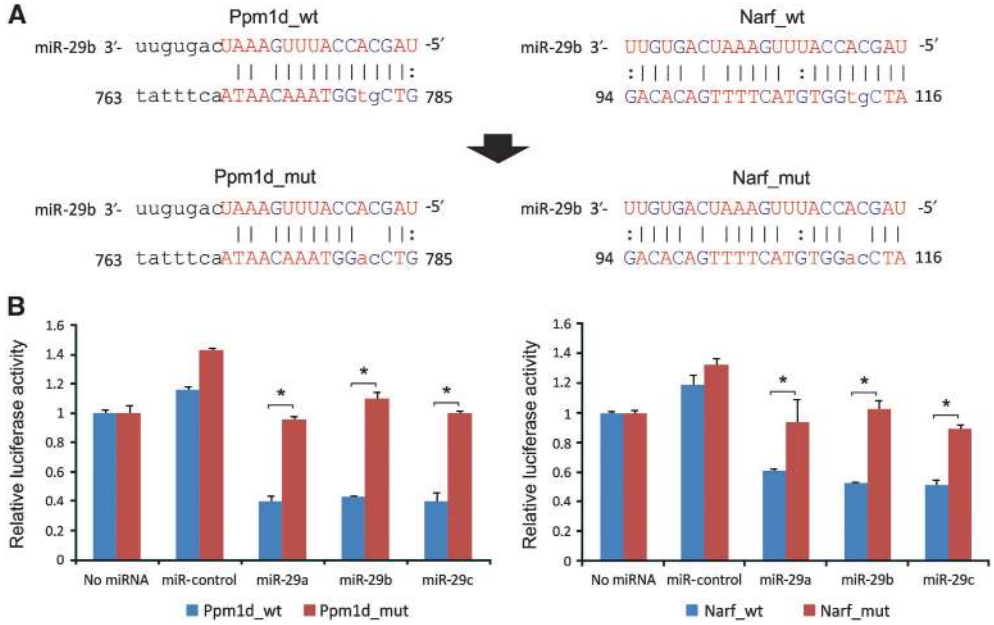

Figure 5 Mutation of the miRNA binding site abolishes miRNA repression. (**A**) Pairwise alignment between miR-29b and the wild-type and mutated 3′-UTR of *Narf* and *Ppm1d* (Narf_mut and Ppm1d_mut), in which bases at positions 4 and 5 of the seed region were mutated and are highlighted in grey. (**B**) Luciferase experiments with the wild-type and the mutated 3′-UTR of *Narf* and *Ppm1d*. Mutation of the seed region of the 3′-UTR binding site abolishes the repression triggered by either of the three miR-29 miRNAs, confirming the presence of functional miRNA binding sites in the 3′-UTR of *Narf* and *Ppm1d*. *Significantly different, $P<0.05$.

Watson–Crick miRNA–mRNA complementarity within the seed region of the binding site was sufficient to abolish the repression effect caused by any of the three miR-29 miRNAs in luciferase experiments (Figure 5B).

As a different approach to validate these results and place them in the context of the DNA damage response, HEK-293 cells transfected with the *Ppm1d* and *Narf* luciferase constructs were treated for 24 h with doxorubicin, and the luminescence emission was assayed (Figure 6A and B). Doxorubicin treatment strongly repressed the luminescence emission of cells transfected with the wild-type *Ppm1d* and *Narf* 3′-UTRs compared with untreated cells. In contrast, transfection of miR-29 inhibitory molecules (anti-miR 29) together with the 3′-UTRs of these targets abolished (Figure 6A) or significantly reverted (Figure 6B) the translational repression induced by doxorubicin. Several studies have reported the influence of mRNA structure in the miRNA-mediated repression. To rule out any interference of the mRNA structure and visualize the translational repression at the protein level, we extended the above analysis to the complete mRNA of *Ppm1d* and *Narf* genes, including the 3′-UTR. To achieve this goal, we cloned the complete *Ppm1d* and *Narf* mRNAs in a mammalian expression vector and transfected each of them with either a mixture of the three miR-29 miRNAs or a control miRNA (Figure 6C and D). In both cases, protein synthesis resulted strongly inhibited when miR-29 miRNAs were present, thereby confirming the functionality of the miR-29 binding sites predicted within the 3′-UTR of *Ppm1d* and *Narf*. On the basis of these results, we conclude that the DNA damage response can mediate the repression of these targets through members of the miR-29 family of miRNAs.

Finally, and also in relation to the identified targets of miR-29 in cells from *Zmpste24* progeroid mice, it is remarkable that a comparative analysis of the skeletal muscle transcriptome of *Zmpste24*$^{-/-}$ mice (Varela *et al*, 2005) with expression levels of predicted miR-29 targets demonstrated significant overlap in the analysed data sets (Supplementary Figure S1B). Further, RT–PCR expression analysis of genes such as *Ppm1d, Hbp1* and *Narf*, which were not represented in the available transcriptomic data, revealed a clear downregulation of *Narf* expression levels and no significant changes in *Hbp1* and *Ppm1d* mRNA levels, although a trend towards downregulation in the mutant tissues was observed for all transcripts (Supplementary Figure S1C).

miR-29 family reduces proliferation and enhances cell senescence

Among the selected miR-29 targets of potential relevance in aging processes, we focused our attention on the Ppm1d/Wip1 phosphatase, since it has been previously reported that this protein is a key regulator of the DNA damage response through its ability to dephosphorylate a wide variety of proteins such as p53, Chk1, Chk2, p38, γ-H2AX and ATM (Lu *et al*, 2008a; Cha *et al*, 2010). According to this, and given that this family of miRNAs is regulated by the DNA damage response and miR-29 levels are progressively accumulated during cell senescence, we asked whether miR-29 family could modulate cell viability in culture fibroblasts. As a first attempt to evaluate this hypothesis, we transfected three different primary fibroblast cell lines with a combination of miR-29a, -29b and -29c precursor molecules and we measured cell proliferation during three passages by cell counting. As shown in Figure 7A, exogenous addition of miR-29 compromises cell proliferation in primary fibroblasts. In addition, analysis of cell senescence in miR-29 overexpressing fibroblasts demonstrated a consistent accumulation of SA-βGal-positive cells and increased levels of γ-H2AX compared with control cells at the end point of this experi-

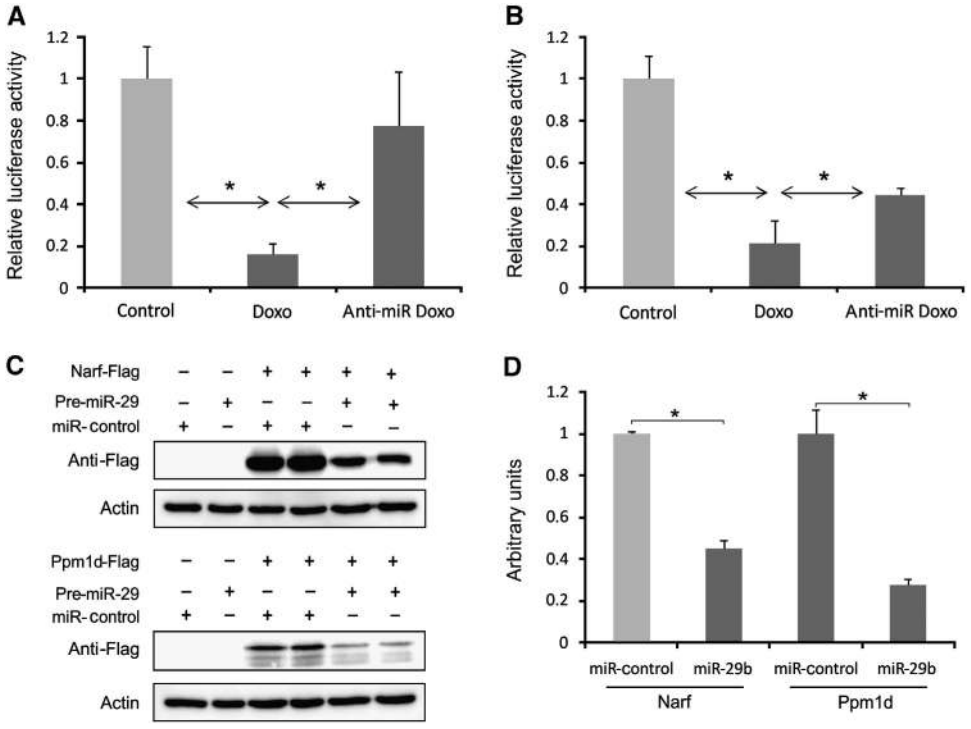

Figure 6 Doxorubicin treatment represses Ppm1d and Narf synthesis through miR-29. Doxorubicin treatment decreases luminescence emission in cells transfected with the wild-type 3′-UTR of *Ppm1d* (**A**) and *Narf* (**B**). Transfection of miR-29 inhibitory molecules abolishes the translational repression over the 3′-UTRs of *Ppm1d* and *Narf* after doxorubicin treatment ($n=3$ biological replicates). (**C**) Immunoblotting of HEK-293 cells transfected with pcDNA-flag-Narf or pcDNA-flag-Ppm1d in combination with miR-29 microRNA precursor molecules or a microRNA control. The full-length mRNAs of both *Narf* and *Ppm1d*, including the 3′-UTR were cloned into pcDNA vector in frame with a flag epitope for immunoblot detection with an anti-Flag antibody. (**D**) Densitometry analysis of the immunoblots shown in (**A**). Overexpression of miR-29 reduces the protein levels of Narf and Wip1 by 55 and 72%, respectively. *Significantly different, $P<0.05$.

ment (Figure 7A). Given these results, we asked whether miR-29 inhibition could delay replicative senescence in *Zmpste24*$^{-/-}$ fibroblasts by transfection of antagomiR molecules against miR-29. As expected, we observed a marked increase in proliferative potential of the anti-miR-29-transfected cell cultures in comparison to scrambled anti-miR-transfected cell lines (Figure 7B). Moreover, anti-miR-29 transfection of *Zmpste24*$^{-/-}$ fibroblasts yielded a significant increase in both the number of senescent and γ-H2AX-positive cells (Figure 7B). To further confirm these results, cell proliferation in wild-type fibroblasts transfected with miR-29 precursor molecules and *Zmpste24*$^{-/-}$ fibroblasts transfected with inhibitor molecules was assessed by MTT assays at different time points (Supplementary Figure S2A). These experiments corroborated and reinforced the previous observations. Additionally, we examined whether augmented miR-29 levels can enhance sensitivity to DNA damage drugs in fibroblasts. To achieve this goal, control or miR-29-transfected fibroblasts were treated with doxorubicin and cell viability was measured using an MTT assay. As shown in Figure 7C, miR-29-transfected fibroblasts were more sensitive to doxorubicin treatment, showing a considerable reduction in cell viability. On the other hand, reduction of miR-29 levels in *Zmpste24*$^{-/-}$ fibroblasts by transfection of anti-miR molecules resulted in augmented cell viability under doxorubicin conditions in comparison to scrambled anti-miR-transfected cells. To confirm that these observations can be extended to other cellular systems, we analysed the impact of miR-29 on the proliferation potential of U2OS human osteosarcoma cells. To achieve this goal, we used a different approach which consists of the overexpression of the miR-29b and -29c levels by using a lentiviral vector that expresses the miR-29b-2∼29c cluster. Consistent with observations in fibroblasts, U2OS cells transduced with the miR-29 lentiviral vector showed a marked reduction in proliferation potential in comparison to cells transduced with the empty vector (Supplementary Figure S2B). Furthermore, we were able to demonstrate that transfection of anti-miR-29 molecules restored the proliferation potential of U2OS cells that overexpress miR-29. Collectively, these results demonstrate that the miR-29 family modulates cell viability through regulation of cell proliferation and senescence, features that perfectly correlate with the phenotype alterations observed in *Zmpste24*$^{-/-}$ progeroid mice.

miR-29 regulates p53 phosphorylation through Ppm1d repression

Since *Ppm1d* is a *bona fide* target of miR-29 and a well-known regulator of p53, we proceeded to analyse the impact of miR-29 on the p53 pathway. For this purpose, wild-type primary fibroblasts were transfected with miR-29 precursors or inhibitory molecules or their corresponding scrambled controls, and p53 phosphorylation was analysed by western blot in both untreated and doxorubicin-treated conditions (Figure 8A). Although in untreated conditions there were no clear differences, we observed a strong correlation in the phosphorylation status of p53 at serine 15—the residue targeted by Ppm1d—and miR-29 levels in doxorubicin-treated

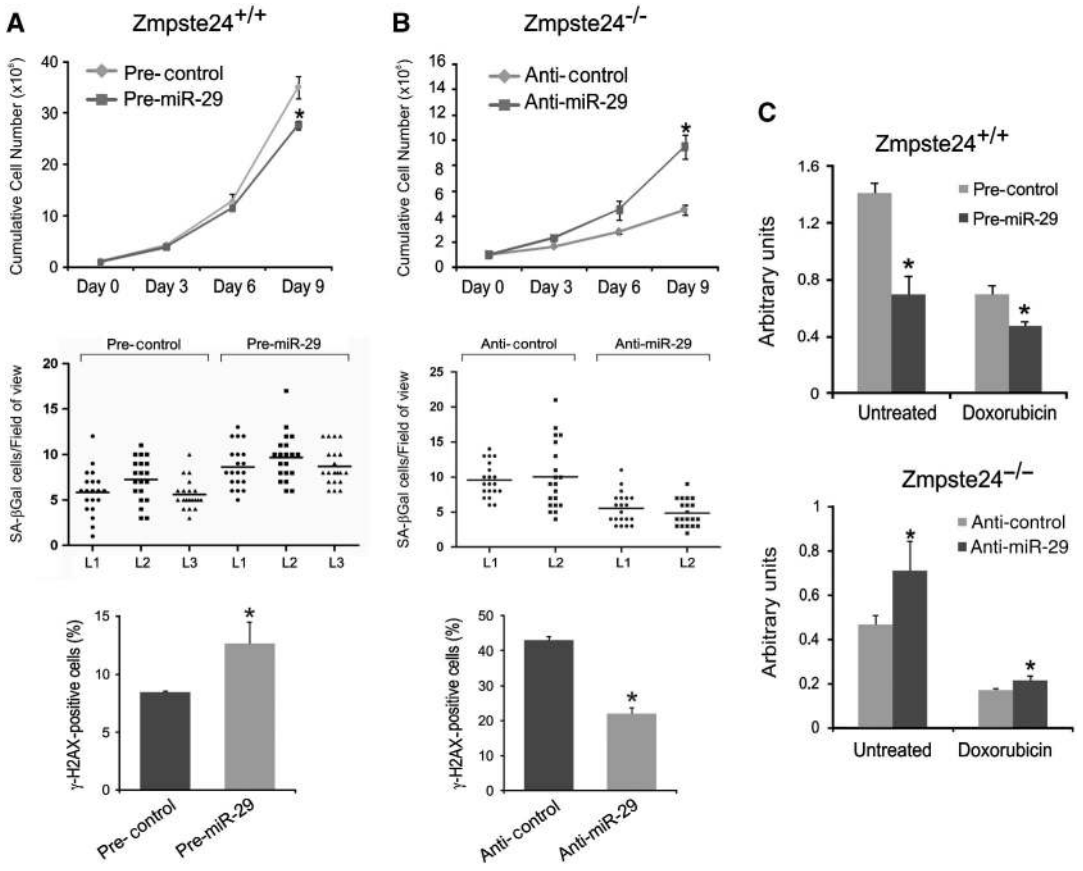

Figure 7 miR-29 overexpression reduces cell proliferation and viability and increases senescence. (**A**) Effects of miR-29 on cell proliferation and senescence. Passage 2 wild-type primary fibroblasts were transfected with a combination of miR-29a, -29b and -29c or control precursor miRNA (pre-miR-29 or pre-control) A million cells growing in 10 cm dishes were transfected with the indicated molecules and every 3 days cell populations were determined by cell counting using a hemocytometer (top panel). At each passage, a million cells were re-seeded and this procedure was repeated during three passages (three wild-type and three mutant mice fibroblasts were used in each condition). Additionally, SA-βGal activity (middle panel) and γ-H2AX (bottom panel) markers at the end point of the experiment were analysed. (**B**) The same experiment was carried out with passage 4 *Zmpste24*$^{-/-}$ fibroblast using inhibitory molecules (anti-miR-29 or anti-control). (**C**) MTT assay of cell viability under doxorubicin treatment. Primary wild-type fibroblasts (top panel) transfected with miR-29 or control precursor molecules and *Zmpste24*-deficient mice fibroblast transfected with miR-29 or control inhibitor molecules (bottom panel) were treated with 1 μM doxorubicin or left untreated for 72 h and cell viability was measured by MTT assay ($n = 3$ biological replicates). *Significantly different from pre- or anti-control transfected cells, $P < 0.05$.

cells. Thus, transfection of precursor molecules resulted in elevated levels of phospho-p53 whereas in anti-miR-transfected fibroblasts, there was a marked reduction in phosphorylated p53. Accordingly, we tried to reduce the phosphorylation levels of p53 in *Zmpste24*$^{-/-}$ fibroblasts by transfection of miR-29 inhibitor molecules (Figure 8B). Interestingly, miR-29 inhibition successfully reduced the levels of phosphorylated p53 in both untreated and doxorubicin-treated cells in comparison to the scrambled anti-miR-transfected cells. Due to antibody specificity limitations, we were unable to perform a reliable measure of Ppm1d protein levels in murine systems. Consequently, we moved to a human system by using U2OS osteosarcoma cells, which display normal PPM1D levels and p53 responsiveness. As shown in Figure 8C, U2OS cells transfected with miR-29 precursor molecules display a strong reduction in PPM1D protein levels, which correlates with an increase in phospho-p53 levels, while total-p53 showed no substantial changes. However, in this system, miR-29 inhibition did not result in consistent changes in *PPM1D* expression, which could be explained by repression by other miRNAs whose expression is altered in this cell line.

To further correlate miR-29 levels with *Ppm1d* repression and p53 phosphorylation, we used a different approach involving infection of U2OS cells with a lentiviral vector expressing the miR-29b-2-c cluster or the empty vector, followed by analysis of the p53 response in both basal and doxorubicin-treatment conditions. As can be seen in Figure 8D, miR-29 expressing cells presented diminished basal levels of PPM1D and higher levels of p53 phosphorylation, and displayed an exacerbated response to DNA damage that also correlates with the PPM1D levels. These results are consistent with previous works describing that miR-29 enhances p53 responsiveness through p53 stabilization, which agrees well with our results since phosphorylation stabilizes this tumour suppressor protein and prevents its proteasome-mediated degradation (Lavin and Gueven, 2006).

Discussion

Since the discovery of miRNA-mediated translational regulation, a wide variety of functions have been associated with this process. Compared with protein–protein interactions, in which a single protein interacts with a reduced number of

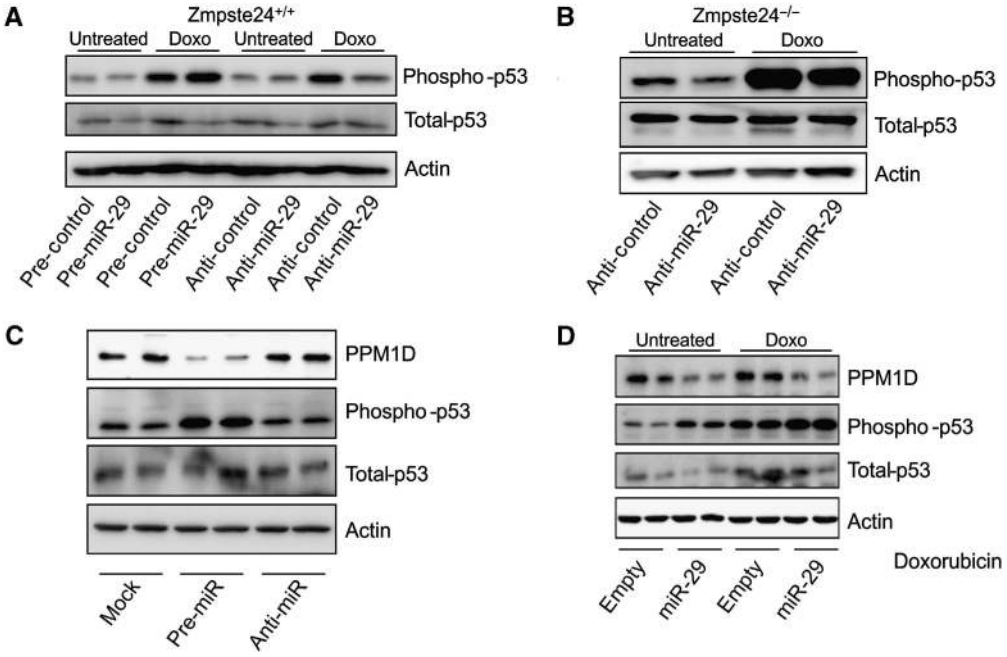

Figure 8 miR-29 modulates the DNA damage response through Ppm1d. (**A**) Wild-type mouse ear fibroblasts were transfected with a combination of pre- or anti-miR-29 molecules, left to recover for 24 h and treated with 0.5 μM doxorubicin or left untreated for 24 h. Then, cells were harvested and phospho-(S15)-p53, total-p53 and β-actin protein levels were analysed by western blot using specific antibodies. (**B**) Western blot of *Zmpste24*$^{-/-}$ primary fibroblasts transfected with control or miR-29 inhibitor molecules in untreated or doxorubicin-treated conditions. After transfection, cells were left to recover for 24 h, and then treated with 0.5 μM doxorubicin or left untreated for 24 h. (**C**) Western blot analysis of U2OS cells transfected with a combination of pre-miR-29 or anti-miR-29 molecules. After 48 h, transfection cells were harvested and protein levels were assessed by western blot using anti-PPM1D, anti-phospho-(S15)-p53, anti-total-p53 and anti-β-actin antibodies. (**D**) Western blot analysis of U2OS cells infected with a lentiviral vector that expresses miR-29-b-c (miR-29) cluster or the empty vector (empty). Cells were treated with 0.1 μM doxorubicin for 90 min and after 3 h cells were harvested and proteins were separated on SDS–PAGE and probed with anti-PPM1D, anti-phospho-(S15)-p53, anti-total-p53 and anti-β-actin antibodies.

proteins, each miRNA has the potential ability to repress the translation of hundreds of transcripts (Grigoriev, 2003; Lewis *et al*, 2005). Accordingly, dysregulation of miRNA expression could also contribute to the numerous alterations present in a very complex and multifactorial process such as aging. Previous works have analysed the expression of miRNAs in different tissues from young and old mice (Williams *et al*, 2007; Maes *et al*, 2008) as well as in mice with delayed aging (Bates *et al*, 2010), but the role of miRNAs in mice with accelerated aging is still unknown. Our results show that *Zmpste24*-deficient mice, a mouse model of human Hutchinson–Gilford progeria, display dysregulated miRNA expression in liver and muscle. Among those miRNAs whose expression is altered in these progeroid mice, we have identified three miRNAs belonging to the miR-29 family which are significantly overexpressed in tissues from *Zmpste24*$^{-/-}$ mice. miR-29 upregulation was especially relevant in muscle from *Zmpste24*$^{-/-}$ mice, showing up to ~10-fold higher levels than those of control animals. Further studies of miR-29 levels in liver and muscle samples from old mice demonstrated that the changes observed in these premature aging mice also occur during physiological aging. Notably, a recent exhaustive study of the age-related miRNA changes in the human and macaque brain cortex has identified the miR-29 family among those miRNAs with high age-correlated expression (Somel *et al*, 2010). Additionally, miR-29 levels are downregulated in Ames dwarf mice, which display a delay in the onset of aging (Bates *et al*, 2010), thus suggesting a more general role for this miRNA family in the regulation of processes associated with normal and pathological aging.

Functional analysis aimed at the characterization of the molecular mechanisms underlying the observed links between miR-29 and aging has revealed that the miR-29 upregulation is associated with the DNA damage response (Figure 9). We had previously described that tissues from *Zmpste24*-deficient mice present an accumulation of senescent cells and a marked transcriptional activation of p53 downstream targets (Varela *et al*, 2005). Additionally, these progeroid mice present genomic instability and a profound stem cell dysfunction (Liu *et al*, 2005; Espada *et al*, 2008; Marino *et al*, 2008). These previous findings prompted us to consider that the transcriptional activation of *miR-29* family members could be part of the DNA damage response against genomic instability. Consistent with this hypothesis, we have found that miR-29 expression is progressively increased during passage of *Zmpste24*$^{-/-}$ primary cultures from mouse ear fibroblasts, with the highest levels being detected when cells reach replicative senescence. Interestingly, this phenomenon was not an exclusive property of *Zmpste24*-mutant mice fibroblasts, since miR-29 undergoes a similar upregulation in wild-type fibroblasts in serial passage. This observation, together with the finding that both wild-type and mutant mice fibroblasts display similar levels of miR-29 at first passage, indicates that miR-29 changes cannot fully explain the proliferation differences between wild-type and mutant fibroblasts in cell culture. However, the increased levels of senescence and DNA damage markers during serial passage

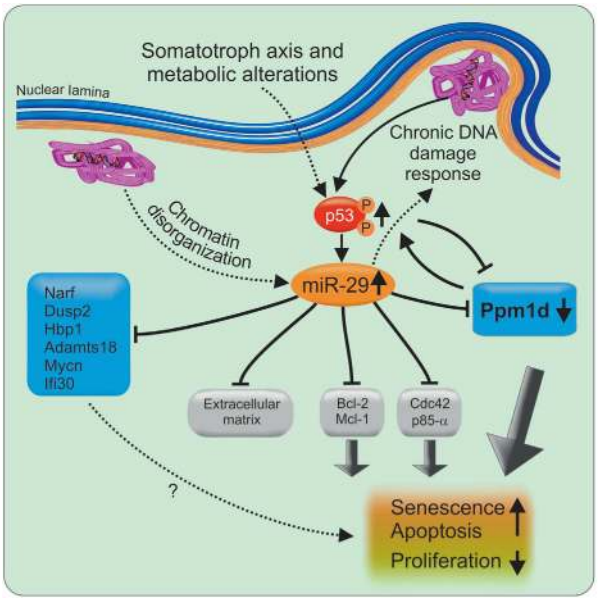

Figure 9 Model for the miR-29 regulatory network in *Zmpste24*$^{-/-}$ progeroid mice. Nuclear lamina alterations of *Zmpste24*$^{-/-}$ cells induce a genomic instability situation that it is recognized by these cells as a chronic DNA damage, thereby activating the p53 signalling pathway. Additionally, nuclear lamina abnormalities disrupt the chromatin–lamina attachment patterns causing profound changes in chromatin structure. These alterations, putatively reinforced by the somatotroph axis and metabolic alterations present in these mice (dotted line), lead to an abnormal miR-29 activation and a subsequent repression of their target genes. These targets include several genes with pro-survival roles, like *Bcl-2*, *Mcl-1*, *Cdc42*, *p85-α* and *Ppm1d/Wip1*, whose downregulation leads to a decrease of cell proliferation and an increase of cell senescence and apoptosis, processes that finally result in the loss of tissue and organism homoeostasis. Moreover, Ppm1d repression diminishes the ratio of p53 dephosphorylation, which positively feedbacks the p53 loop, exacerbating the initial situation. Additionally, increased miR-29 levels may directly participate in further exacerbating DNA damage. Dotted lines indicate hypothetical links.

of both wild-type and mutant mice, although at different extent, link the genotoxic stress with the progressive accumulation of miR-29.

Further confirmation of this association came from the treatment of wild-type fibroblasts with different genotoxic drugs. These experiments have revealed that doxorubicin, a DNA topoisomerase inhibitor that causes double-strand breaks and generates a kind of chronic DNA damage, also induces the transcriptional activation of either miR-29a, -29b, and -29c, in contrast with the treatment with H_2O_2 or 4-NQO, which induce transient oxidative damage or UV-like lesions, respectively. According to these results, only the chronic or difficult to repair DNA damage induces the expression of this family of miRNAs. Furthermore, we have found that this upregulation occurs in a p53-dependent manner, since *p53*$^{-/-}$ murine fibroblasts failed to increase miR-29 expression during successive cell culture passages and upon doxorubicin treatment. Likewise, *ATM*-deficient and *ATR-Seckel* murine fibroblasts failed to induce miR-29 expression when using equivalent concentrations of doxorubicin, which further confirms the link between DNA damage response and miR-29 regulation. More interestingly, high concentrations of doxorubicin activated the expression of miR-29 in both *ATM*-deficient and *ATR-Seckel* fibroblasts, which suggests that other regulatory mechanisms could be operating depending on the extent of DNA damage. In this regard, two recent works have identified c-myc and NF-κB as repressor factors of these miRNAs (Liu *et al*, 2010; Mott *et al*, 2010). Collectively, all these data associate the miR-29 family upregulation present in both *Zmpste24*-deficient mice and normal aging with the DNA damage response activation.

To identify miR-29 targets which could contribute to the observed effects related to aging and DNA damage response in *Zmpste24*$^{-/-}$ progeroid mice, we followed an experimental approach based on the combination of target prediction by different algorithms with luciferase-based validation assays of the predicted targets. This strategy led us to identify seven transcripts subjected to repression by miR-29a, -29b or -29c. Interestingly, we did not observe different repression ratios by any of the three miRNAs of the miR-29 family, which suggests that they are not specialized in different functions and may perform redundant activities in the regulation of the identified targets. These targets include protein phosphatases (Ppm1d/Wip1 and Dusp2), oncogenes (Mycn), interferon-inducible proteins (Ifi30), transcriptional repressors (Hbp1), nuclear envelope proteins (Narf) and metalloproteases (Adamts18). Among all of them, we focused on Ppm1d phosphatase and prelamin A interacting protein Narf, which had been previously associated with processes of interest in relation to DNA damage and aging. Thus, Ppm1d dephosphorylates a variety of proteins involved in DNA damage response, such as p53, Chk1, Chk2, p38, γ-H2AX and ATM (Lu *et al*, 2008a; Cha *et al*, 2010). Moreover, *Ppm1d* is transcriptionally activated by p53 upon DNA damage and participates in a negative regulatory feedback with ATM (Batchelor *et al*, 2008, 2009). On the other hand, Narf interacts with prelamin A, whose accumulation at the nuclear envelope of *Zmpste24*$^{-/-}$ cells is the pathological hallmark underlying the accelerated aging process exhibited by these mice (Varela *et al*, 2008). Consequently, we evaluated the presence of miR-29 binding sites in these two targets, with the finding that a 2-nt mutation in the putative seed sequences of *Ppm1d* and *Narf* 3′-UTR abolishes the translational repression by miR-29 in luciferase assays. We also found that co-expression of the full-length mRNA of *Ppm1d* or *Narf* together with *miR-29* precursor molecules in HEK-293 cells, significantly reduces Narf and Ppm1d protein levels compared with cells transfected with a control miRNA. These experiments confirm that *Ppm1d* and *Narf* transcripts contain functional miR-29 binding sites and that these miRNAs repress the translation of both targets. The lack of appropriate antibodies for Narf precluded further work to explore miR-29 effects on the endogenous protein, but parallel experiments demonstrated that miR-29 family members are able to inhibit endogenous Ppm1d protein production and that this effect has a special impact on the phosphorylation of p53.

According to the above results, it was tempting to speculate that miR-29 upregulation, as a likely consequence of the progressive accumulation of DNA damage, reduces Ppm1d protein levels, a key regulatory phosphatase of the DNA damage response that dephosphorylates a wide variety of proteins such as p53, Chk1, Chk2, p38, γ-H2AX and ATM, important for the control of cell viability (Lu *et al*, 2008a; Cha *et al*, 2010; Le Guezennec and Bulavin, 2010). Experiments aimed to further evaluate this hypothesis confirmed that increased levels of miR-29 through transfection of

miRNA precursor molecules reduce fibroblasts proliferation and enhance cell senescence. Furthermore, γ-H2AX levels were increased in these cells, which demonstrated the increased sensitivity to DNA damage, an observation that was also confirmed by MTT assays of wild-type fibroblasts transfected with miR-29 precursor, although the possibility of a positive feedback in which miR-29 increases DNA damage cannot be discarded (Figure 9). Importantly, we were also able to reverse the proliferation defects in *Zmpste24*$^{-/-}$ fibroblasts by the transfection of antagomiR molecules against miR-29. Thus, miR-29 inhibition in these cells resulted in a strong increase in proliferation potential accompanied by a significant decrease in both the number of SA-βGal- and γ-H2AX-positive cells. Likewise, we could demonstrate that the sensitivity of *Zmpste24*$^{-/-}$ fibroblasts to doxorubicin treatment is significantly diminished when miR-29 is downregulated by transfection of miRNA inhibitor molecules. Also in agreement with our proposal of a role for miR-29 in the modulation of cell viability, we have found higher phosphorylation levels of p53 at Ser15—the residue targeted by Ppm1d—in mouse fibroblasts transfected with miR-29 precursor molecules. Conversely, inhibitory molecules against miR-29 yielded the opposite effect, decreasing the levels of p53 phosphorylation in doxorubicin-treated wild-type fibroblasts. Moreover, a similar experiment with *Zmpste24*-deficient mouse fibroblasts showed that miR-29 inhibition decrease the levels of phosphorylated p53 in both basal and doxorubicin conditions. Furthermore, we were able to correlate the p53 phosphorylation status with the PPM1D protein levels in basal and doxorubicin-treated U2OS human cells. These results are also consistent with previous data showing that miR-29 induces apoptosis in a p53-dependent manner and increases the levels of total-p53 (Park *et al*, 2009), because p53 phosphorylation stabilizes the protein preventing its degradation by the proteasome (Lavin and Gueven, 2006). Likewise, the observation that Ppm1d dephosphorylates Mdm2 and prevents p53 proteasome degradation (Lu *et al*, 2008b), is consistent with our finding that miR-29 targets *Ppm1d* and influences levels and activity of the p53 tumour suppressor.

Collectively, these data together with additional observations from the literature, strongly support our proposal that miR-29 is an aging-related miRNA. First, several reports have described a tumour suppressor role for miR-29 family members in several human cancers including haematological malignancies, rhabdomyosarcoma, pleural mesothelioma and hepatocellular carcinoma (Pekarsky *et al*, 2006; Wang *et al*, 2008; Garzon *et al*, 2009b; Pass *et al*, 2010; Xiong *et al*, 2010; Zhao *et al*, 2010). This tumour suppressive function of miR-29 family members is consistent with a pro-aging role for them, since a growing number of tumour suppressor genes have a negative role during aging through a process known as antagonistic pleiotropy (Campisi, 2005; Kirkwood, 2005). In fact, *Zmpste24*$^{-/-}$ progeroid mice exhibit a chronic hyperactivation of p53 signalling as well as a marked overexpression of other tumour suppressors such as p16/INK4A (Varela *et al*, 2005; Espada *et al*, 2008). Moreover, functions attributed to miR-29 include reduction of cell proliferation and induction of apoptosis, two features associated with the diminished capacity to maintain tissue homoeostasis which is a characteristic feature of aging processes (Mott *et al*, 2007; Muniyappa *et al*, 2009). Notably, it has also been reported that miR-29b induces global DNA hypomethylation by targeting different demethylases (Garzon *et al*, 2009b), another observation that links miR-29 functions and aging, since epigenetic alterations are characteristic features of the aging process (Gravina and Vijg, 2010; Osorio *et al*, 2010). Finally, miR-29 family members show increased expression during aging and an inverse relationship with expression levels of a group of cancer-related genes in human and macaque brain (Somel *et al*, 2010).

In conclusion, we propose that miR-29 has a pivotal role in the regulation of cell survival and proliferation through the modulation of the DNA damage response (Figure 9); thus, making these miRNAs very interesting in the context of both cancer and aging. Disruption of the DNA damage response is a hallmark of cancer progression that is achieved by many tumours through mutations in p53. However, tumours can amplify PPM1D as an alternative way to inhibit p53 activity and, interestingly, these tumours rarely harbour p53 mutations (Bulavin *et al*, 2002). According to our results, miR-29 downregulation could constitute another way for tumours to reduce p53 signalling, thus allowing tumours to escape from apoptosis and growth arrest. Finally, the observation that miR-29 accumulates during aging provides an additional evidence for the implication of miRNAs in the development of the complex process of aging.

Materials and methods

Transgenic animals

Mutant mice deficient in Zmpste24 metalloproteinase have been previously described (Pendas *et al*, 2002). *ATM*$^{-/-}$ and *ATR*$^{s/s}$ mice were kindly provided by Dr Oscar Fernandez-Capetillo (CNIO, Madrid, Spain), and *XPF*$^{-/-}$ and *CSB/XPA*$^{-/-}$ mice by Dr Jan Hoeijmakers (Erasmus University, Rotterdam, The Netherlands). Animal experiments were conducted in accordance with the guidelines of the Committee on Animal Experimentation of the Universidad de Oviedo, Oviedo, Spain.

Luciferase assays

For miR-29 target validation, the entire 3′-UTR murine sequence of each predicted target gene was PCR amplified and cloned into psiCHECK-2 plasmid (kindly provided by Dr A Rodriguez, The Welcome Trust Sanger Institute, Cambridge, UK) downstream of the Renilla luciferase ORF using the restriction enzymes *Xho*I and *Not*I. HEK-293 cells were seeded 6 h before transfection in 24-well plates at 50% of confluence. Transfections were performed using lipofectamine 2000 (Invitrogen), 250 ng of each psiCHECK-2 constructs and 20 pmol of miR-29a, -29b, -29c or control miRNA molecules (Ambion), following the manufacturer's instructions. Transfection was carried out for 4 h, and then medium was removed and cells were left to recover for 18 h. For promoter analysis, the indicated genomic regions of each cluster were cloned into pGL3-basic plasmid (Promega) using the restriction enzyme *Sma*I. In all, 250 ng of the resulting plasmids was transfected in HCT-116 cells growing in 24-well plates in combination with 12.5 ng of the pRLTK plasmid (Promega) using lipofectamine 2000 (Invitrogen). Transfections were carried out for 4 h, and then medium was replaced by fresh medium alone or containing 0.5 μM doxorubicin, 0.5 μM 4-nitroquinolone-1-oxide or 20 μM H_2O_2. Determination of luciferase activity was performed using Dual-luciferase® Reporter Assay System (Promega). Briefly, cells on 24-well plates were washed with PBS and lysed by pipetting mixing using 80 μl of the passive lysis buffer. Then, both Renilla and Firefly luciferase activity of each sample were measured in a TD-20/20 luminometer (Turner Biosystems).

Immunoblotting analysis

Cell cultures were washed with PBS and homogenized in an appropriate volume of 20 mM Tris buffer pH 7.4, containing 150 mM NaCl, 1% Triton X-100, 10 mM EDTA, Complete® protease inhibitor cocktail (Roche Applied Science), and phosphatase inhibitors

(200 μM sodium orthovanadate, 1 mM β-glycerophosphate). Once homogenized, cell extracts were sonicated and subsequently centrifuged at 12 000 *g* at 4°C, with the resulting supernatants being collected. The protein concentration of the supernatant was evaluated by bicinchoninic acid (BCA protein assay kit, Pierce Biotechnology, Rockford, IL) and 4 μg of each cell extract was loaded onto SDS–polyacrylamide gels. After electrophoresis, gels were electrotransferred onto nitrocellulose membranes, and then the membranes were blocked with 5% non-fat dried milk in PBT (phosphate buffered saline with 0.05% Tween-20) and incubated with primary antibodies in 5% BSA in PBT. After three washes with PBT, membranes were incubated with horseradish peroxidase-conjugated goat anti-rabbit IgG at a 1:10 000 dilution in 1.5% milk in PBT, and developed with a West Pico enhanced chemiluminescence kit (Pierce Biotechnology). For immunoblotting, the following antibodies were used: anti-PPM1D (Bethyl Laboratories), anti-S15-phospho-p53 (Cell Signaling), anti-total-p53 (Cell Signaling), anti-flag (Sigma-Aldrich) and anti-β-actin (Sigma-Aldrich).

microRNA analysis

microRNA profiling was performed as previously described (Lu *et al*, 2005) using total RNA extracted with TRIzol (Invitrogen). For qPCR analysis, total RNA was prepared using miRVANA™ miRNA isolation Kit (Ambion, Austin, TX) and RNA samples were quantified and evaluated for purity (260 nm/280 nm ratio) using a NanoDrop ND-1000 spectrophotometer. miRNA detection was performed using Taqman® miRNA expression assays (Applied Biosystems). Briefly, 10 ng of total RNA was reverse transcribed using Taqman® miRNA reverse transcription kit (Applied Biosystems) and PCR amplified using an Applied Biosystems 7300 Real-Time PCR system. As an internal control, miRNA expression was normalized to snoRNA202 for mouse samples and to RNU6B for human samples, using Taqman® Gene Expression Assays (Applied Biosystems). All protocols were carried out according to the manufacturer's instructions.

Cell culture

HCT-116 cells were kindly provided by Dr B Vogelstein (Ludwig Center, Baltimore, MD, USA), HEK-293T and U2OS cells by Dr PP Durán (CNIO) and p53-deficient cells by Dr M Serrano (CNIO). Cultures were maintained in Dulbecco's modified Eagle's medium (DMEM, Gibco) supplemented with 10% fetal bovine serum (FBS) and 1% penicillin–streptomycin–glutamine (Gibco). Murine fibroblasts were extracted from 12-week-old mice ears. Ears were sterilized with ethanol, washed with PBS, and triturated with razor blades. Samples were then incubated with 600 μl of 4 mg/ml collagenase D (Roche) and 4 mg/ml dispase II (Roche) in DMEM for 45 min at 37°C and 5% CO_2. After filtering and washing, 6 ml of DMEM with 10% FBS and 1% antibiotic-antimycotic were added, and the mixture was incubated at 37°C and 5% CO_2. Cell numbers were determined using a hemocytometry and 10^6 cells were passed into a 10-cm plate every 3 days and cultured under standard conditions. For DNA damage induction, cells were seeded in 6-well plates and after 24 h, doxorubicin (Sigma) was added to the growing media. After a 24-h period, RNA was extracted and microRNA expression was analysed. Cell counting was performed using a Bright-Line hemacytometer (Hausser Scientific) following the manufacturer's instructions.

Cell transfections

Transfection of the U2OS cell line was carried out using lipofectamine RNAiMAX (Invitrogen) following manufacturer's instructions. U2OS cells were seeded in 6-well plates and the miRNA precursor or inhibitory molecules (from Dharmacon Inc) were transfected at a final concentration of 25 nM. For primary fibroblast transfections, two rounds of consecutive transfections were performed using lipofectamine RNAiMAX. miRNA inhibition was carried out using a control or miR-29b mercury LNA™ power inhibitors from Exiqon at a final concentration of 20 nM. miRNA over-expression in fibroblasts was performed using a mixture of miR-29a, -29b and -29c or control precursor molecules from Dharmacon Inc at a final concentration of 25 nM.

Viral package and cell infection

Lentiviruses were packaged in HEK-293T cells using a VSVG-based package system kindly provided by Dr JM Silva (Columbia University, New York, USA). Cells were seeded in 6-well plates 24 h before transfection. The next day, cells were transfected using TransIT®-LT1 Transfection Reagent (Mirus) and a mixture of 2 μg of the desired plasmid and 1 μg of each lentiviral helper, following the manufacturer's instructions. Transfection medium was removed 24 h after transfection and fresh medium was added to the plate. Cell supernatants were collected at 24 and 48 h, cleared by centrifugation at 1200 r.p.m. for 10 min and filtered through a 0.45-μm sterile filter. U2OS cells were seeded in 6-well plate at 20–30% confluence 24 h before the infection. The following day, 1 ml of viral supernatant was added to growing media supplemented with 5 μg/ml of polybrene (Millipore), centrifuged at 1000 r.p.m. for 1 h at room temperature and incubated for 8 h. This step was repeated twice and cells were left recovering for 24 h in growing media before drug selection. Cells infected with pLemiR or pMSCV constructs were selected with 2 μg/ml of puromycin (Sigma) or 100 μg/ml of hygromycin (Invitrogen), respectively.

Cell senescence analysis

Cell senescence was assessed by detecting the senescence-associated β-galactosidase activity at pH 6.0 (SA-βGal) using the Senescence β-galactosidase kit from Cell Signaling. Staining was performed in 6-well plates and the SA-βGal-positive cells were detected by phase contrast microscopy using a Zeiss Axiovert 200M fluorescence microscope (Zeiss). Quantification was performed by counting the positive cells present in 20 independent fields of view at ×10 magnification, and images were captured and processed using Adobe Photoshop CS3 and displayed using CorelDraw.

Immunofluorescence

Cells were seeded on glass coverslips, allowed to recover for 24 h and then fixed for 10 min at room temperature in 4% p-formaldehyde-buffered solution, followed by permeabilization with 0.5% Triton X-100 for 5 min. Cell preparations were blocked for 45 min at room temperature in 0.5% bovine serum albumin in PBS. Cells were incubated with anti-γH2AX antibody (1:250, Millipore) overnight at 4°C, and then with the appropriate fluorescence-conjugated secondary antibodies (Invitrogen) for 1 h at room temperature. Nuclei were stained by incubating cells with 4′,6-diamidino-2-phenylindole (DAPI), after which, coverslips were mounted on slides and cells imaged with a Zeiss Axiovert 200M fluorescence microscope (Zeiss). Images were processed using Adobe Photoshop CS3 and displayed using CorelDraw.

MTT assay

For MTT assay, 2500 fibroblasts or 5000 U2OS cells per well were seeded in 96-well plates. Transfection of miRNA precursor or inhibitor molecules was performed at the time of seeding using lipofectamine RNAiMAX (Invitrogen) according to the reverse protocol provided by the manufacturer. After transfection, medium was changed and MTT assay was performed at different time points using the Cell Titer 96 Non-Radioactive Cell Proliferation Assay (Promega). At each time point, 15 μl of dye solution was added to the medium for 2 h followed by an addition of 100 μl of solubilization solution. After 1 h incubation at 37°C, absorbance at 570 nm was measured using a powerWave XS spectrophotometer (Biotek).

Statistical and bioinformatics analysis

For computational prediction of the miR-29 targets, a combination of the following software was used: TargetScan (http://www.targetscan.org), Microcosm (http://www.ebi.ac.uk/enright-srv/microcosm/htdocs/targets/v5/) and PicTar (http://pictar.mdc-berlin.de/). All experimental data are reported as mean values and the error bars represent the s.e.m.. Statistical analysis was performed by the non-parametric Student's *t* test, using the Prism program v4.0 (GraphPad software, Inc).

Supplementary data

Supplementary data are available at *The EMBO Journal* Online (http://www.embojournal.org).

Acknowledgements

We thank M Fernández and C Garabaya for excellent technical assistance and Drs J Hoeijmakers, B Vogelstein, PP Durán, M Serrano,

JM Silva and O Fernández-Capetillo for providing cells, tissues and reagents. This work has been supported by grants from Ministerio de Ciencia e Innovación-Spain and European Union (FP7 MicroEnviMet). The Instituto Universitario de Oncología is supported by Obra Social Cajastur and Acción Transversal del Cáncer-RTICC. JR is supported by a fellowship from Fundación María Cristina Masaveu Peterson. CLO is an Investigator of the Botín Foundation.

Author contributions: APU designed and carried out most of the experiments and co-wrote the paper. AJR performed and analysed the immunofluorescence and SA-βGAL assays, collaborated in the promoter experiments and co-wrote the paper. JRS carried out some of the qPCR experiments and luciferase assays. IV provided mice biopsies and advised in cell culture. GM advised in immunoblotting experiments and experimental design. JC collaborated in the microRNA profiling and experimental design. JL carried out the microRNA profiling. JMPF analysed most data and advised in some experiments. CLO conceived and supervised the work and co-wrote the paper.

Conflict of interest

The authors declare that they have no conflict of interest.

References

Batchelor E, Loewer A, Lahav G (2009) The ups and downs of p53: understanding protein dynamics in single cells. *Nat Rev Cancer* **9:** 371–377

Batchelor E, Mock CS, Bhan I, Loewer A, Lahav G (2008) Recurrent initiation: a mechanism for triggering p53 pulses in response to DNA damage. *Mol Cell* **30:** 277–289

Bates DJ, Li N, Liang R, Sarojini H, An J, Masternak MM, Bartke A, Wang E (2010) MicroRNA regulation in Ames dwarf mouse liver may contribute to delayed aging. *Aging Cell* **9:** 1–18

Boehm M, Slack F (2005) A developmental timing microRNA and its target regulate life span in C. elegans. *Science* **310:** 1954–1957

Broers JL, Ramaekers FC, Bonne G, Yaou RB, Hutchison CJ (2006) Nuclear lamins: laminopathies and their role in premature ageing. *Physiol Rev* **86:** 967–1008

Bulavin DV, Demidov ON, Saito S, Kauraniemi P, Phillips C, Amundson SA, Ambrosino C, Sauter G, Nebreda AR, Anderson CW, Kallioniemi A, Fornace Jr AJ, Appella E (2002) Amplification of PPM1D in human tumors abrogates p53 tumor-suppressor activity. *Nat Genet* **31:** 210–215

Bushati N, Cohen SM (2007) microRNA functions. *Annu Rev Cell Dev Biol* **23:** 175–205

Cadinanos J, Varela I, Lopez-Otin C, Freije JM (2005) From immature lamin to premature aging: molecular pathways and therapeutic opportunities. *Cell Cycle* **4:** 1732–1735

Campisi J (2005) Aging, tumor suppression and cancer: high wire-act!. *Mech Ageing Dev* **126:** 51–58

Cha H, Lowe JM, Li H, Lee JS, Belova GI, Bulavin DV, Fornace Jr AJ (2010) Wip1 directly dephosphorylates gamma-H2AX and attenuates the DNA damage response. *Cancer Res* **70:** 4112–4122

Drummond MJ, McCarthy JJ, Fry CS, Esser KA, Rasmussen BB (2008) Aging differentially affects human skeletal muscle microRNA expression at rest and after an anabolic stimulus of resistance exercise and essential amino acids. *Am J Physiol Endocrinol Metab* **295:** E1333–E1340

Elson A, Wang Y, Daugherty CJ, Morton CC, Zhou F, Campos-Torres J, Leder P (1996) Pleiotropic defects in ataxia-telangiectasia protein-deficient mice. *Proc Natl Acad Sci USA* **93:** 13084–13089

Eller MS, Ostrom K, Gilchrest BA (1996) DNA damage enhances melanogenesis. *Proc Natl Acad Sci USA* **93:** 1087–1092

Espada J, Varela I, Flores I, Ugalde AP, Cadinanos J, Pendas AM, Stewart CL, Tryggvason K, Blasco MA, Freije JM, Lopez-Otin C (2008) Nuclear envelope defects cause stem cell dysfunction in premature-aging mice. *J Cell Biol* **181:** 27–35

Flynt AS, Lai EC (2008) Biological principles of microRNA-mediated regulation: shared themes amid diversity. *Nat Rev Genet* **9:** 831–842

Garzon R, Calin GA, Croce CM (2009a) MicroRNAs in cancer. *Annu Rev Med* **60:** 167–179

Garzon R, Liu S, Fabbri M, Liu Z, Heaphy CE, Callegari E, Schwind S, Pang J, Yu J, Muthusamy N, Havelange V, Volinia S, Blum W, Rush LJ, Perrotti D, Andreeff M, Bloomfield CD, Byrd JC, Chan K, Wu LC *et al* (2009b) MicroRNA-29b induces global DNA hypomethylation and tumor suppressor gene reexpression in acute myeloid leukemia by targeting directly DNMT3A and 3B and indirectly DNMT1. *Blood* **113:** 6411–6418

Gravina S, Vijg J (2010) Epigenetic factors in aging and longevity. *Pflugers Arch* **459:** 247–258

Grigoriev A (2003) On the number of protein-protein interactions in the yeast proteome. *Nucleic Acids Res* **31:** 4157–4161

Harvey M, Sands AT, Weiss RS, Hegi ME, Wiseman RW, Pantazis P, Giovanella BC, Tainsky MA, Bradley A, Donehower LA (1993) *In vitro* growth characteristics of embryo fibroblasts isolated from p53-deficient mice. *Oncogene* **8:** 2457–2467

Hasty P, Campisi J, Hoeijmakers J, van Steeg H, Vijg J (2003) Aging and genome maintenance: lessons from the mouse? *Science* **299:** 1355–1359

He L, He X, Lowe SW, Hannon GJ (2007) microRNAs join the p53 network–another piece in the tumour-suppression puzzle. *Nat Rev Cancer* **7:** 819–822

Hoeijmakers JH (2009) DNA damage, aging, and cancer. *N Engl J Med* **361:** 1475–1485

Kirkwood TB (2005) Understanding the odd science of aging. *Cell* **120:** 437–447

L'Ecuyer T, Sanjeev S, Thomas R, Novak R, Das L, Campbell W, Heide RV (2006) DNA damage is an early event in doxorubicin-induced cardiac myocyte death. *Am J Physiol Heart Circ Physiol* **291:** H1273–H1280

Lavin MF, Gueven N (2006) The complexity of p53 stabilization and activation. *Cell Death Differ* **13:** 941–950

Le Guezennec X, Bulavin DV (2010) WIP1 phosphatase at the crossroads of cancer and aging. *Trends Biochem Sci* **35:** 109–114

Lewis BP, Burge CB, Bartel DP (2005) Conserved seed pairing, often flanked by adenosines, indicates that thousands of human genes are microRNA targets. *Cell* **120:** 15–20

Liu B, Wang J, Chan KM, Tjia WM, Deng W, Guan X, Huang JD, Li KM, Chau PY, Chen DJ, Pei D, Pendas AM, Cadinanos J, Lopez-Otin C, Tse HF, Hutchison C, Chen J, Cao Y, Cheah KS, Tryggvason K *et al* (2005) Genomic instability in laminopathy-based premature aging. *Nat Med* **11:** 780–785

Liu S, Wu LC, Pang J, Santhanam R, Schwind S, Wu YZ, Hickey CJ, Yu J, Becker H, Maharry K, Radmacher MD, Li C, Whitman SP, Mishra A, Stauffer N, Eiring AM, Briesewitz R, Baiocchi RA, Chan KK, Paschka P *et al* (2010) Sp1/NFkappaB/HDAC/miR-29b regulatory network in KIT-driven myeloid leukemia. *Cancer Cell* **17:** 333–347

Lu J, Getz G, Miska EA, Alvarez-Saavedra E, Lamb J, Peck D, Sweet-Cordero A, Ebert BL, Mak RH, Ferrando AA, Downing JR, Jacks T, Horvitz HR, Golub TR (2005) MicroRNA expression profiles classify human cancers. *Nature* **435:** 834–838

Lu X, Nguyen TA, Moon SH, Darlington Y, Sommer M, Donehower LA (2008a) The type 2C phosphatase Wip1: an oncogenic regulator of tumor suppressor and DNA damage response pathways. *Cancer Metastasis Rev* **27:** 123–135

Lu X, Nguyen TA, Zhang X, Donehower LA (2008b) The Wip1 phosphatase and Mdm2: cracking the "Wip" on p53 stability. *Cell Cycle* **7:** 164–168

Maes OC, An J, Sarojini H, Wang E (2008) Murine microRNAs implicated in liver functions and aging process. *Mech Ageing Dev* **129:** 534–541

Marino G, Ugalde AP, Salvador-Montoliu N, Varela I, Quiros PM, Cadinanos J, van der Pluijm I, Freije JM, Lopez-Otin C (2008) Premature aging in mice activates a systemic metabolic response involving autophagy induction. *Hum Mol Genet* **17:** 2196–2211

Mott JL, Kobayashi S, Bronk SF, Gores GJ (2007) mir-29 regulates Mcl-1 protein expression and apoptosis. *Oncogene* **26:** 6133–6140

Mott JL, Kurita S, Cazanave SC, Bronk SF, Werneburg NW, Fernandez-Zapico ME (2010) Transcriptional suppression of mir-29b-1/mir-29a promoter by c-Myc, hedgehog, and NF-kappaB. *J Cell Biochem* **110:** 1155–1164

Muniyappa MK, Dowling P, Henry M, Meleady P, Doolan P, Gammell P, Clynes M, Barron N (2009) MiRNA-29a regulates the expression of numerous proteins and reduces the invasiveness and proliferation of human carcinoma cell lines. *Eur J Cancer* **45:** 3104–3118

Murga M, Bunting S, Montana MF, Soria R, Mulero F, Canamero M, Lee Y, McKinnon PJ, Nussenzweig A, Fernandez-Capetillo O (2009) A mouse model of ATR-Seckel shows embryonic replicative stress and accelerated aging. *Nat Genet* **41:** 891–898

Osorio FG, Obaya AJ, Lopez-Otin C, Freije JM (2009) Accelerated ageing: from mechanism to therapy through animal models. *Transgenic Res* **18:** 7–15

Osorio FG, Varela I, Lara E, Puente XS, Espada J, Santoro R, Freije JM, Fraga MF, Lopez-Otin C (2010) Nuclear envelope alterations generate an aging-like epigenetic pattern in mice deficient in Zmpste24 metalloprotease. *Aging Cell* **9:** 947–957

Park SY, Lee JH, Ha M, Nam JW, Kim VN (2009) miR-29 miRNAs activate p53 by targeting p85 alpha and CDC42. *Nat Struct Mol Biol* **16:** 23–29

Pass HI, Goparaju C, Ivanov S, Donington J, Carbone M, Hoshen M, Cohen D, Chajut A, Rosenwald S, Dan H, Benjamin S, Aharonov R (2010) hsa-miR-29c* is linked to the prognosis of malignant pleural mesothelioma. *Cancer Res* **70:** 1916–1924

Pekarsky Y, Santanam U, Cimmino A, Palamarchuk A, Efanov A, Maximov V, Volinia S, Alder H, Liu CG, Rassenti L, Calin GA, Hagan JP, Kipps T, Croce CM (2006) Tcl1 expression in chronic lymphocytic leukemia is regulated by miR-29 and miR-181. *Cancer Res* **66:** 11590–11593

Pendas AM, Zhou Z, Cadinanos J, Freije JM, Wang J, Hultenby K, Astudillo A, Wernerson A, Rodriguez F, Tryggvason K, Lopez-Otin C (2002) Defective prelamin A processing and muscular and adipocyte alterations in Zmpste24 metalloproteinase-deficient mice. *Nat Genet* **31:** 94–99

Rokhlin OW, Scheinker VS, Taghiyev AF, Bumcrot D, Glover RA, Cohen MB (2008) MicroRNA-34 mediates AR-dependent p53-induced apoptosis in prostate cancer. *Cancer Biol Ther* **7:** 1288–1296

Shenouda SK, Alahari SK (2009) MicroRNA function in cancer: oncogene or a tumor suppressor? *Cancer Metastasis Rev* **28:** 369–378

Somel M, Guo S, Fu N, Yan Z, Hu HY, Xu Y, Yuan Y, Ning Z, Hu Y, Menzel C, Hu H, Lachmann M, Zeng R, Chen W, Khaitovich P (2010) MicroRNA, mRNA, and protein expression link development and aging in human and macaque brain. *Genome Res* **20:** 1207–1218

Tarasov V, Jung P, Verdoodt B, Lodygin D, Epanchintsev A, Menssen A, Meister G, Hermeking H (2007) Differential regulation of microRNAs by p53 revealed by massively parallel sequencing: miR-34a is a p53 target that induces apoptosis and G1-arrest. *Cell Cycle* **6:** 1586–1593

Tian M, Shinkura R, Shinkura N, Alt FW (2004) Growth retardation, early death, and DNA repair defects in mice deficient for the nucleotide excision repair enzyme XPF. *Mol Cell Biol* **24:** 1200–1205

van der Pluijm I, Garinis GA, Brandt RM, Gorgels TG, Wijnhoven SW, Diderich KE, de Wit J, Mitchell JR, van Oostrom C, Beems R, Niedernhofer LJ, Velasco S, Friedberg EC, Tanaka K, van Steeg H, Hoeijmakers JH, van der Horst GT (2007) Impaired genome maintenance suppresses the growth hormone–insulin-like growth factor 1 axis in mice with Cockayne syndrome. *PLoS Biol* **5:** e2

Varela I, Cadinanos J, Pendas AM, Gutierrez-Fernandez A, Folgueras AR, Sanchez LM, Zhou Z, Rodriguez FJ, Stewart CL, Vega JA, Tryggvason K, Freije JM, Lopez-Otin C (2005) Accelerated ageing in mice deficient in Zmpste24 protease is linked to p53 signalling activation. *Nature* **437:** 564–568

Varela I, Pereira S, Ugalde AP, Navarro CL, Suarez MF, Cau P, Cadinanos J, Osorio FG, Foray N, Cobo J, de Carlos F, Levy N, Freije JM, Lopez-Otin C (2008) Combined treatment with statins and aminobisphosphonates extends longevity in a mouse model of human premature aging. *Nat Med* **14:** 767–772

Vijg J, Campisi J (2008) Puzzles, promises and a cure for ageing. *Nature* **454:** 1065–1071

Wang H, Garzon R, Sun H, Ladner KJ, Singh R, Dahlman J, Cheng A, Hall BM, Qualman SJ, Chandler DS, Croce CM, Guttridge DC (2008) NF-kappaB-YY1-miR-29 regulatory circuitry in skeletal myogenesis and rhabdomyosarcoma. *Cancer Cell* **14:** 369–381

Williams AE, Perry MM, Moschos SA, Lindsay MA (2007) microRNA expression in the aging mouse lung. *BMC Genomics* **8:** 172

Xiong Y, Fang JH, Yun JP, Yang J, Zhang Y, Jia WH, Zhuang SM (2010) Effects of microRNA-29 on apoptosis, tumorigenicity, and prognosis of hepatocellular carcinoma. *Hepatology* **51:** 836–845

Zhao JJ, Lin J, Lwin T, Yang H, Guo J, Kong W, Dessureault S, Moscinski LC, Rezania D, Dalton WS, Sotomayor E, Tao J, Cheng JQ (2010) microRNA expression profile and identification of miR-29 as a prognostic marker and pathogenetic factor by targeting CDK6 in mantle cell lymphoma. *Blood* **115:** 2630–2639

